

# Reconstruction of the Antenna Far-Field Pattern through a Fast Plane-Polar Scanning

F. D'Agostino, F. Ferrara, C. Gennarelli, R. Guerriero, and M. Migliozi

Dipartimento di Ingegneria Industriale  
University of Salerno, via Giovanni Paolo II, 132 - 84084 Fisciano, Italy  
fdagostino@unisa.it, flferrara@unisa.it, cgennarelli@unisa.it, rguerriero@unisa.it, mmigliozi@unisa.it

**Abstract** — This paper provides the experimental validation of a fast and accurate technique, which allows the reconstruction of the antenna radiation pattern from a minimum number of near-field measurements collected through a plane-polar scanning. This near-field to far-field (NFTFF) transformation technique relies on a nonredundant sampling representation of the voltage acquired by the probe, achieved by modeling the antenna with a double bowl, a very flexible model particularly suitable to deal with antennas having a quasi-planar geometry. The NF data required by the standard plane-rectangular NFTFF transformation are efficiently reconstructed from the nonredundant plane-polar ones by using an optimal sampling interpolation algorithm, thus making possible to get a considerable measurement time saving. The accuracy and practical efficacy of the described technique are assessed by experimental tests carried out at the Antenna Characterization Lab of the University of Salerno.

**Index Terms** — Antenna measurements, nonredundant sampling representations, plane-polar near-field to far-field transformation.

## I. INTRODUCTION

Since the beginning of 70s, near-field to far-field (NFTFF) transformation techniques [1-6] are a widely employed and recognized tool for the precise measurement of the FF radiation characteristics of antennas, whose sizes in terms of wavelengths do not allow the fulfillment of the Fraunhofer distance requirements in an anechoic chamber. Among these techniques, the standard NFTFF with plane-rectangular scanning [7, 8] can be conveniently employed when measuring high gain antennas exhibiting pencil beam radiation patterns. For this kind of antennas, a convenient and appealing alternative to such a classical transformation is that using the plane-polar scanning [9-11]. Such a scan (see Fig. 1) is simpler than the plane-rectangular one from the mechanical point of view, since it involves a linear displacement of the probe and a rotation of the antenna under test (AUT). Other advantages are: a larger measurement zone as compared

with the plane-rectangular scanning case, for a fixed extent of the anechoic chamber; a “fine chamber tuning”, because the AUT always points in the same direction; a more accurate testing of gravitationally sensitive spaceborne antennas [9], since the scanning can be easily accomplished in a horizontal plane. However, in the former approach [9, 10], the antenna far-field was evaluated by employing a Jacobi-Bessel expansion, so that a large computational time was needed. Such a drawback has been surmounted in [11], by reconstructing the NF data required to perform the standard plane-rectangular NFTFF transformation from the collected plane-polar ones, through a very simple bivariate Lagrange interpolation formula. This has made possible the exploitation of the fast Fourier transform (FFT) algorithm to efficiently reconstruct the antenna far-field. Unfortunately, because of the generic nature of such an interpolation formula, very close spacings were required to minimize the interpolation error. A more effective interpolation algorithm, requiring a significantly lower number of data with respect to the previous approaches [9-11], has been developed in [12], by properly taking into account that the radiated or scattered electromagnetic (EM) fields are spatially quasi-bandlimited functions [13] and employing the optimal sampling interpolation (OSI) expansions, able to minimize the truncation error for a fixed number of nearest considered samples.

The measurement time reduction is nowadays one of the hottest issues related to the NFTFF transformation techniques, since the time required to acquire the NF data is remarkably greater than the computer time needed to perform the NFTFF transformation. To this end, the nonredundant sampling representations of EM fields [14, 15] have been usefully applied to develop NFTFF transformations with plane-rectangular [16, 17] and plane-polar scans [18, 19] using a minimum number of NF measurements. In particular, the fast and accurate sampling representation, which allows the efficient reconstruction of the near-field data required by the standard plane-rectangular NFTFF transformation from the acquired plane-polar samples, has been obtained by considering the AUT as enclosed in a “double bowl” [18]

or in an oblate ellipsoid [19]. Both these representations contain as particular case that relevant to the spherical modeling [20], but, when considering quasi-planar antennas, they allow to obtain a further reduction of the required NF data number and to locate the scanning plane at a distance less than one half of the antenna maximum dimension, thus lowering the error due to the truncation of the measurement zone. In fact, according to the nonredundant representations [14], the observation surface must be external to the surface modeling the AUT. It is worthy to note that the sample spacings required by the nonredundant approaches [18-20] are larger than those derived in [21, 22] by a rigorous sampling theorem in plane-polar coordinates.

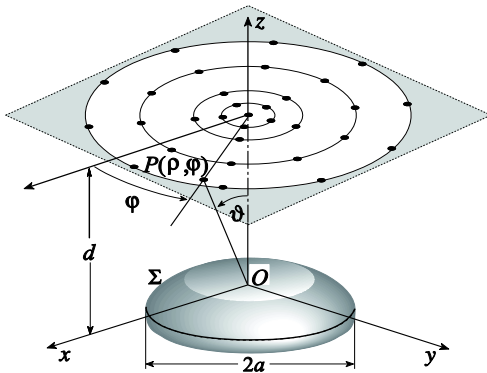


Fig. 1. Plane-polar scanning.

The aim of this paper is to experimentally validate the nonredundant NFFFT transformation with plane-polar scan, adopting a double bowl to model an antenna with a quasi-planar geometry. The experimental tests have been performed in the Antenna Characterization Lab of the University of Salerno, equipped with a plane-polar NF scanning system. It is worth noting that the experimental validation of the NFFFT transformation based on the oblate ellipsoidal modeling of the AUT has been already provided in [23].

## II. NONREDUNDANT PROBE VOLTAGE REPRESENTATION ON A PLANE

Let an AUT be considered as contained in a rotational surface  $\Sigma$  delimiting a convex domain and the voltage be acquired by a nondirective probe on a plane at  $z = d$ , where  $(x, y, z)$  is a Cartesian coordinate system with the origin at the AUT centre (Fig. 1). A spherical reference system  $(r, \theta, \varphi)$  is used for denoting any observation point, whereas a point  $P$  lying on the plane can be also specified by the plane-polar coordinates  $(\rho, \varphi)$ . The nonredundant sampling representations of EM fields [14] can be applied to the probe voltage  $V$ , since the voltage acquired by a nondirective probe is characterized by the same effective spatial bandwidth of the antenna field [24]. Accordingly, it is advantageous to describe each of the curves  $C$  (radial

lines and rings), representing the plane in a plane-polar frame, in terms of an optimal parameter  $\xi$  and to define the “reduced voltage”:

$$\tilde{V}(\xi) = V(\xi)e^{j\gamma(\xi)}, \quad (1)$$

wherein  $V(\xi)$  is the voltage acquired by the probe ( $V_\varphi$ ) or the probe rotated by  $90^\circ$  around its longitudinal axis ( $V_\rho$ ) and  $\gamma(\xi)$  is a proper phase factor. The error resulting when approximating  $\tilde{V}(\xi)$  by a bandlimited function can be effectively reduced by imposing that this function has a properly increased bandwidth  $\chi'W_\xi$ , with  $W_\xi$  being a critical value and  $\chi' > 1$  the excess bandwidth factor [14].

When considering a radial line, the bandwidth  $W_\xi$ , the parameterization  $\xi$  and the corresponding phase function  $\gamma$  are [14]:

$$W_\xi = \beta \ell' / 2\pi, \quad (2)$$

$$\gamma = (\beta/2) [R_1 + R_2 + s'_1 - s'_2], \quad (3)$$

$$\xi = (\pi/\ell') [R_1 - R_2 + s'_1 + s'_2], \quad (4)$$

wherein  $\ell'$  is the length of the intersection curve  $C'$  between the meridian plane passing through the observation point  $P$  and  $\Sigma$ ,  $\beta$  is the wavenumber,  $R_{1,2}$  are the distances from  $P$  to the two tangency points  $P_{1,2}$  between  $C'$  and the cone having the vertex at  $P$ , and  $s'_{1,2}$  their curvilinear abscissas.

When the curve  $C$  is a ring, the angle  $\varphi$  can be conveniently adopted as optimal parameter, whereas  $\gamma$  is constant. The related bandwidth  $W_\varphi$  is [14]:

$$W_\varphi = \frac{\beta}{2} \max_{z'} (R^+ - R^-) = \frac{\beta}{2} \max_{z'} \left( \sqrt{(\rho + \rho'(z'))^2 + (z - z')^2} - \sqrt{(\rho - \rho'(z'))^2 + (z - z')^2} \right), \quad (5)$$

where  $\rho'(z')$  specifies the surface  $\Sigma$  and  $R^+, R^-$  are the maximum and minimum distances of  $C$  from the circumference of  $\Sigma$  at  $z'$ . As shown in [14], the maximum is achieved on that zone of  $\Sigma$ , which lies on the same side of  $C$  with respect to its maximum transverse circumference.

According to the theoretical results in [14], the surface  $\Sigma$  must fit very well the AUT shape in order to minimize the number of needed samples. The antennas characterized by using a planar NF scanning system have usually a quasi-planar geometry, so that an oblate ellipsoid [19, 23] or a “double bowl” [18] can be conveniently employed as AUT models to get effective sampling representations on the plane. Although these models are particularly tailored for quasi-planar antennas, they are quite general and contain the spherical modeling as particular case. The choice of which of them has to be adopted to shape a given AUT depends only on the modeling which better fits its actual geometry.

The nonredundant sampling representation using the “double bowl” modeling is detailed in the following. The double bowl is a surface consisting of two circular bowls with the same aperture radius  $a$ , but with radii  $h$  and  $h'$  of

the upper and lower arcs which may differ for a better fitting of the actual AUT geometry (Figs. 1 and 2). The bandwidth, the parameterization, and the phase function relevant to a radial line are obtained from relations (2) – (4) by taking into account that  $\ell' = 2[b + b' + (h + h')\pi/2]$  and substituting in them the appropriate values of  $R_{1,2}$  and  $s'_{1,2}$  [18]. It is easy to verify that, for  $\rho < a$ , the tangency points  $P_{1,2}$  are both situated on the upper bowl (Fig. 2 (a)) and it results [18]:

$$R_1 = \sqrt{d^2 - h^2 + (\rho + b)^2}; \quad s'_1 = -(b + h\alpha_1), \quad (6)$$

$$\alpha_1 = \tan^{-1}(R_1/h) - \tan^{-1}[(\rho + b)/d], \quad (7)$$

$$R_2 = \sqrt{d^2 - h^2 + (b - \rho)^2}; \quad s'_2 = b + h\alpha_2, \quad (8)$$

$$\alpha_2 = \tan^{-1}(R_2/h) - \tan^{-1}[(b - \rho)/d], \quad (9)$$

whereas, for  $\rho > a$ ,  $P_2$  is on the lower bowl so that  $R_1$  and  $s'_1$  are still given by (6), while

$$R_2 = \sqrt{d^2 - h^2 + (\rho - b')^2}; \quad s'_2 = b + h\pi/2 + h'\alpha_2, \quad (10)$$

$$\alpha_2 = \tan^{-1}(R_2/h') + \tan^{-1}[(\rho - b')/d] - \pi/2. \quad (11)$$

For what concerns the evaluation of the maximum in relation (5) allowing the determination of  $W_\varphi$ , it is convenient to express  $z'$  and  $\rho'$  in terms of the angle  $\delta$  (Fig. 2 (b)) as  $z' = h \cos \delta$ ,  $\rho' = b + h \sin \delta$ . As shown in [18], such a maximum is the solution of the following equation:

$$bd(\cos^2 \delta - \sin^2 \delta) + [\rho^2 + d^2 - b^2] \sin \delta \cos \delta + \\ -h(b \cos \delta + d \sin \delta) = 0,$$

belonging to the interval  $[0, \pi/2]$ .

In light of the above results, the voltage at any point  $P(\vartheta, \varphi)$  on the plane can be efficiently reconstructed by means of the two-dimensional OSI expansion [18]:

$$V(\xi(\vartheta), \varphi) = e^{-j\gamma(\xi)} \sum_{n=n_0-q+1}^{n_0+q} \left\{ A(\xi, \xi_n, \bar{\xi}, N, N'') \cdot \right. \\ \left. \sum_{m=m_0-p+1}^{m_0+p} \tilde{V}(\xi_n, \varphi_{m,n}) A(\varphi, \varphi_{m,n}, \bar{\varphi}, M_n, M_n'') \right\}, \quad (12)$$

where  $2q \times 2p$  is the number of retained reduced voltage samples  $\tilde{V}(\xi_n, \varphi_{m,n})$ ,  $n_0 = \text{Int}(\xi/\Delta\xi)$ ,  $m_0 = \text{Int}(\varphi/\Delta\varphi_n)$ ,  $\xi_n = n\Delta\xi = 2\pi n/(2N''+1)$ ;  $N'' = \text{Int}(\chi N') + 1$ , (13)

$$N' = \text{Int}(\chi' W_\xi) + 1; \quad N = N'' - N'; \quad \bar{\xi} = q\Delta\xi, \quad (14)$$

$$\varphi_{m,n} = m\Delta\varphi_n = 2\pi m/(2M_n''+1); \quad M_n'' = \text{Int}(\chi M_n') + 1, \quad (15)$$

$$M_n' = \text{Int}[\chi^* W_\varphi(\xi_n)] + 1; \quad M_n = M_n'' - M_n', \quad (16)$$

$$\chi^* = 1 + (\chi' - 1) [\sin \vartheta(\xi_n)]^{-2/3}; \quad \bar{\varphi} = p\Delta\varphi_n, \quad (17)$$

$\chi$  is an oversampling factor controlling the truncation error [14],  $\text{Int}(x)$  denotes the integer part of  $x$ , and

$$A(\alpha, \alpha_\ell, \bar{\alpha}, L, L'') = \Omega_L(\alpha - \alpha_\ell, \bar{\alpha}) D_L''(\alpha - \alpha_\ell), \quad (18)$$

is the OSI interpolation function. Moreover,

$$D_L''(\alpha) = \frac{\sin[(2L''+1)\alpha/2]}{(2L''+1)\sin(\alpha/2)}, \quad (19)$$

and

$$\Omega_L(\alpha, \bar{\alpha}) = \frac{T_L[2\cos^2(\alpha/2)/\cos^2(\bar{\alpha}/2) - 1]}{T_L[2/\cos^2(\bar{\alpha}/2) - 1]}, \quad (20)$$

are the Dirichlet and Tschebyscheff sampling functions [14],  $T_L(\alpha)$  being the Tschebyscheff polynomial of degree  $L$ .

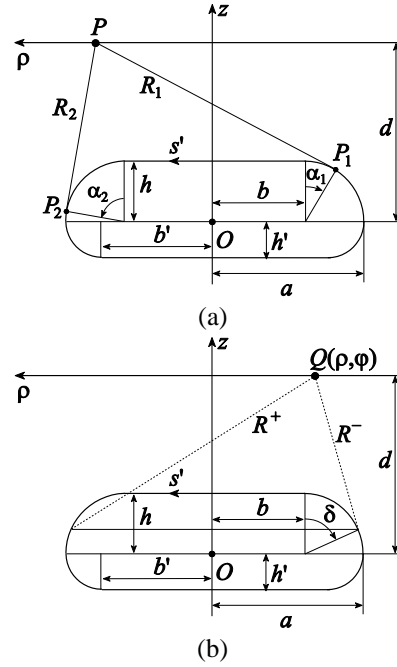


Fig. 2. Double bowl modeling: (a) relevant to the evaluation of  $\gamma$  and  $\xi$ , (b) relevant to the evaluation of  $W_\varphi$ .

It must be stressed that the two-dimensional OSI expansion (12) has the interesting features to reduce the truncation error for a given number of retained samples and to avoid the propagation of the errors affecting the samples [12, 18]. Accordingly, it can be properly exploited to accurately recover the voltages  $V_\varphi$  and  $V_\rho$  at any point in the measurement circle and, in particular, at those needed by the classical probe compensated NFFTF transformation with plane-rectangular scanning [8]. Unfortunately, the probe corrected formulas in [8] (whose expressions in the here adopted reference system are shown in the next section) are valid as long as the probe maintains its orientation with respect to the AUT and this requires its co-rotation with it. A probe having a far-field characterized by a first-order  $\varphi$ -dependence can be properly used for avoiding such a co-rotation. As a matter of fact, in this case, the voltages  $V_V$  and  $V_H$  (acquired with co-rotation by the probe and rotated probe) can be

determined from  $V_\varphi$  and  $V_\rho$  as follows:

$$V_V = V_\varphi \cos \varphi - V_\rho \sin \varphi; \quad V_H = V_\varphi \sin \varphi + V_\rho \cos \varphi. \quad (21)$$

### III. PLANE-RECTANGULAR NFFTF TRANSFORMATION

For reader's convenience, this section reports the key formulas of the probe-corrected NFFTF transformation with plane-rectangular scanning [8], particularized for the here considered reference system (see Fig. 1) when an open-ended rectangular waveguide is adopted as measurement probe.

As shown in [7, 8], by properly applying the Lorentz reciprocity theorem and the plane wave spectrum representation of EM fields, the antenna far-field components  $E_g$ ,  $E_\varphi$  are related to the two-dimensional Fourier transforms  $I_V$ ,  $I_H$  of the output probe voltages  $V_V$ ,  $V_H$  and to the far-field components  $E'_{g_V}$ ,  $E'_{\varphi_V}$  and  $E'_{g_H}$ ,  $E'_{\varphi_H}$  of the electric field radiated by the probe and the probe rotated by  $90^\circ$ , when operating in the transmitting mode, by the following expressions:

$$E_g(\vartheta, \varphi) = (I_H E'_{\varphi_V}(\vartheta, -\varphi) - I_V E'_{\varphi_H}(\vartheta, -\varphi)) / \Delta, \quad (22)$$

$$E_\varphi(\vartheta, \varphi) = (I_H E'_{g_V}(\vartheta, -\varphi) - I_V E'_{g_H}(\vartheta, -\varphi)) / \Delta, \quad (23)$$

where

$$\Delta = E'_{g_H}(\vartheta, -\varphi) E'_{\varphi_V}(\vartheta, -\varphi) - E'_{g_V}(\vartheta, -\varphi) E'_{\varphi_H}(\vartheta, -\varphi), \quad (24)$$

$$I_{V,H} = B \cos \vartheta e^{j\beta d \cos \vartheta}.$$

$$\int_{-\infty}^{+\infty} \int_{-\infty}^{+\infty} V_{V,H}(x, y) e^{j\beta x \sin \vartheta \cos \varphi} e^{j\beta y \sin \vartheta \sin \varphi} dx dy, \quad (25)$$

$B$  being an appropriate constant.

As shown in [25], the FF components of the electric field radiated by an  $a' \times b'$  sized open-ended rectangular waveguide, wherein a  $TE_{10}$  mode is propagating, are:

$$E'_{g_V} = f_g(\vartheta) \sin \varphi \frac{e^{-j\beta r}}{r} = A_E \frac{1 + (k_z/\beta) \cos \vartheta}{1 + (k_z/\beta)} \cdot \frac{\sin[\beta(b'/2) \sin \vartheta]}{\beta(b'/2) \sin \vartheta} \sin \varphi \frac{e^{-j\beta r}}{r}, \quad (26)$$

$$E'_{\varphi_V} = f_\varphi(\vartheta) \cos \varphi \frac{e^{-j\beta r}}{r} = A_H \cos[\beta(a'/2) \sin \vartheta] \cdot \left\{ \frac{\cos \vartheta + (k_z/\beta) + \Gamma[\cos \vartheta - (k_z/\beta)]}{(\pi/2)^2 - [\beta(a'/2) \sin \vartheta]^2} + C_0 \right\} \cos \varphi \frac{e^{-j\beta r}}{r}, \quad (27)$$

where

$$A_E = A_H \left\{ \frac{4}{\pi^2} [1 + (k_z/\beta) + \Gamma(1 - (k_z/\beta))] + C_0 \right\}, \quad (28)$$

$$A_H = -j \beta^2 a' b' E_0 / 8, \quad (29)$$

$k_z = [\beta^2 - (\pi/a')^2]^{1/2}$  is the propagation constant of the  $TE_{10}$  mode,  $E_0$  is its amplitude, and  $\Gamma$  is the reflection

coefficient at the end of the waveguide, whose measured values are shown in [25]. Moreover,  $C_0$  is a real constant that can be numerically computed as described in [25]. The FF components of the electric field radiated by the rotated probe can be easily determined by straightforward evaluations, thus getting:

$$E'_{g_H} = f_g(\vartheta) \cos \varphi \frac{e^{-j\beta r}}{r}, \quad (30)$$

$$E'_{\varphi_H} = -f_\varphi(\vartheta) \sin \varphi \frac{e^{-j\beta r}}{r}. \quad (31)$$

### IV. EXPERIMENTAL TESTING

Some experimental results validating the efficacy of the described nonredundant NFFTF transformation with plane-polar scanning are shown in this section. The experimental proofs have been carried out in the anechoic chamber ( $8\text{m} \times 5\text{m} \times 4\text{m}$  sized) of the Antenna Characterization Lab of the University of Salerno, covered by pyramidal absorbers ensuring a reflectivity lower than  $-40$  dB and equipped with a NF plane-polar scanning system, besides the cylindrical and spherical ones. The plane-polar scanning is achieved by mounting the AUT on a rotator and the probe (an open-ended WR90 rectangular waveguide) on a linear vertical scanner. A vector network analyzer is used to perform the amplitude and phase measurements of the voltages acquired by the probe. The employed AUT is a dual pyramidal horn antenna with horizontal polarization, placed on the plane  $z = 0$  and operating at 10 GHz. The horns have a  $8.9\text{cm} \times 6.8\text{cm}$  sized aperture and the distance between the apertures centers is 26 cm. A photo of the plane-polar NF facility with the dual pyramidal horn antenna is reported in Fig. 3. Note that, in order to show the roll positioner and the AUT mounting, the photo has been taken before covering the rotator and AUT support with the necessary absorbers. The nonredundant plane-polar samples have been collected on a circle having radius 110 cm on a plane 17 cm away from the considered antenna, which has been shaped by a double bowl, whose geometric parameters are  $a = 18.6$  cm and  $h = h' = 2.85$  cm.

The amplitude and phase of the voltage  $V_\varphi$  on the radial line at  $\varphi = 0^\circ$ , recovered from the collected nonredundant plane-polar samples, are compared in Figs. 4 and 5 with the directly measured ones (references). The comparison between the reconstructed amplitude of the voltage  $V_\rho$  on the radial line at  $\varphi = 90^\circ$  and that directly measured is shown in Fig. 6. The reconstructions of the amplitudes of  $V_\varphi$  and  $V_\rho$  on the radial line at  $\varphi = 30^\circ$  are reported in Fig. 7, while that relevant to the phase of  $V_\varphi$  is shown in Fig. 8. All recoveries are resulted to be very good, except for small discrepancies occurring in the zones characterized by very low voltage levels, thus assessing the effectiveness of the OSI formulas. Note that, the recovered voltages show a smoother behavior than the

measured ones, since the spectral content of the noise at the spatial frequencies higher than the antenna spatial band-width are cut away owing to the low pass filtering characteristics of the OSI functions. As regards the choice of the OSI algorithm parameters, the excess bandwidth factor  $\chi'$  has been chosen equal to 1.35 to make negligible the aliasing error with respect to the measurement one, whereas  $\chi = 1.20$  and  $p = q = 7$  have been used to neglect the truncation error [18].

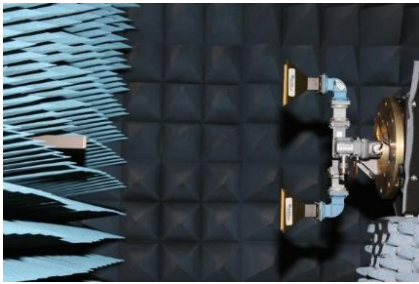


Fig. 3. Photo of the plane-polar NF facility with the dual pyramidal horn antenna.

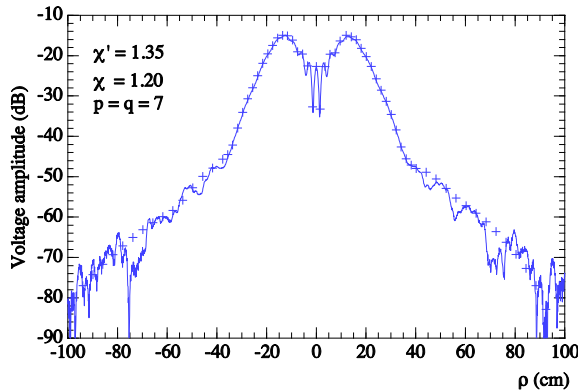


Fig. 4. Amplitude of  $V_\varphi$  on the radial line at  $\varphi = 0^\circ$ . Solid line: reference. Crosses: reconstructed from the nonredundant plane-polar NF samples.

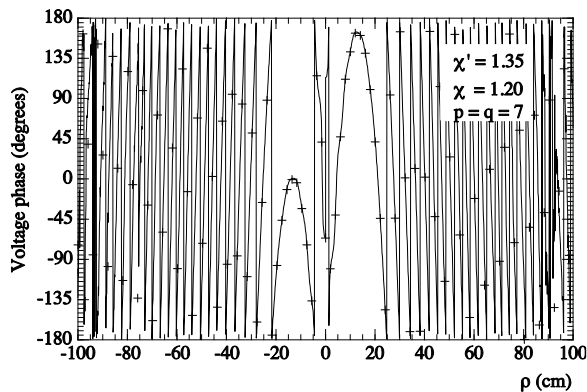


Fig. 5. Phase of  $V_\varphi$  on the radial line at  $\varphi = 0^\circ$ . Solid line: reference. Crosses: reconstructed from the nonredundant plane-polar NF samples.

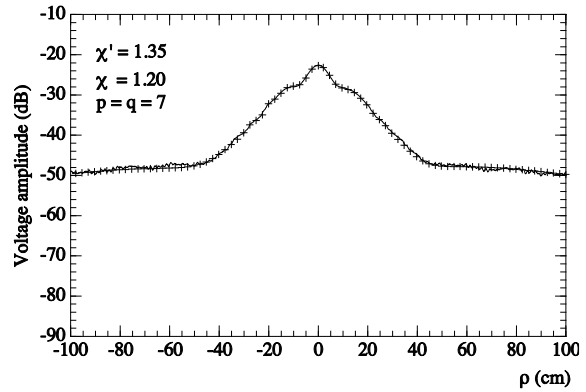


Fig. 6. Amplitude of  $V_\rho$  on the radial line at  $\varphi = 90^\circ$ . Solid line: reference. Crosses: reconstructed from the nonredundant plane-polar NF samples.

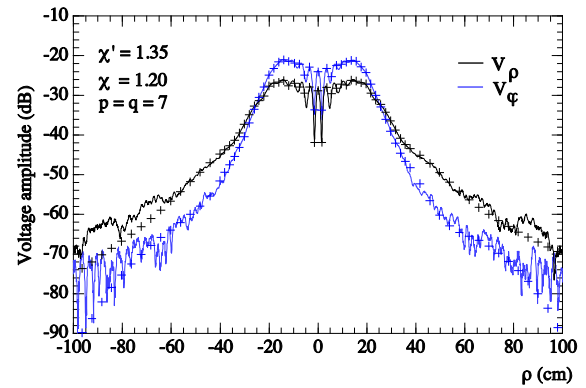


Fig. 7. Amplitudes of  $V_\varphi$ ,  $V_\rho$  on the radial line at  $\varphi = 30^\circ$ . Solid lines: references. Crosses: reconstructed from the nonredundant plane-polar NF samples.

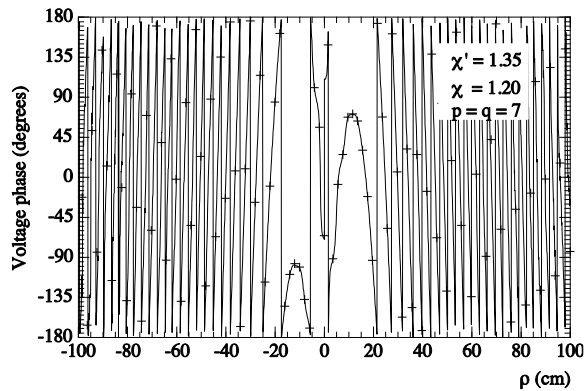


Fig. 8. Phase of  $V_\varphi$  on the radial line at  $\varphi = 30^\circ$ . Solid line: reference. Crosses: reconstructed from the nonredundant plane-polar NF samples.

Finally, the overall efficacy of such a NFTFF transformation technique is validated by comparing the E- and H-planes FF patterns (see Figs. 9 and 10) recovered

from the acquired nonredundant plane-polar samples with the ones attained by using the NF cylindrical scanning system. Also in such a case, a very good agreement is found.

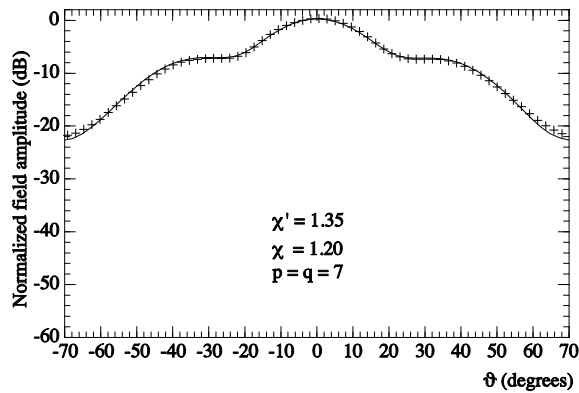


Fig. 9. E-plane pattern. Solid line: reference. Crosses: reconstructed from the nonredundant plane-polar NF samples.

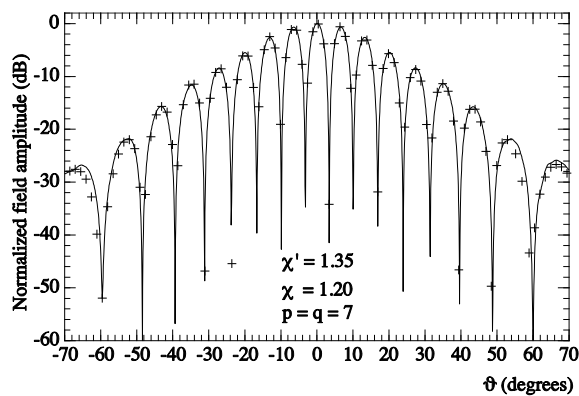


Fig. 10. H-plane pattern. Solid line: reference. Crosses: reconstructed from the nonredundant plane-polar NF samples.

It is noteworthy to compare the acquired NF samples number (1663) with that (33581) needed by the plane-polar scanning techniques [9-11] and with that (21609) required by the classical plane-rectangular NFFTF transformation [8].

The interested reader can find in [26] another set of experimental results relevant to a different AUT, which further assess the effectiveness of the proposed NFFTF transformation technique.

## V. CONCLUSION

The experimental validation of the nonredundant plane-polar NFFTF transformation, using a double bowl to shape the AUT, is provided in this paper. Its effectiveness has been fully confirmed by the very good NF and FF reconstructions. It must be pointed out that the number

of used NF measurements has resulted to be considerably smaller than those required when using the classical NFFTF transformations with plane-rectangular and plane-polar scans, thus showing that such a NFFTF transformation allows a significant measurement time reduction without any loss in accuracy.

## REFERENCES

- [1] A. D. Yaghjian, "An overview of near-field antenna measurements," *IEEE Trans. Antennas Prop.*, vol. AP-34, pp. 30-45, Jan. 1986.
- [2] J. Appel-Hansen, J. D. Dyson, E. S. Gillespie, and T. G. Hickman, *Antenna Measurements*, in *The Handbook of Antenna Design*, A. W. Rudge, K. Milne, A. D. Olver, and P. Knight, Eds., chapter 8, Peter Peregrinus, London, UK 1986.
- [3] E. S. Gillespie, Ed., "Special Issue on near-field scanning techniques," *IEEE Trans. Antennas Prop.*, vol. 36, pp. 727-901, June 1988.
- [4] M. H. Francis and R. W. Wittmann, *Near-Field Scanning Measurements: Theory and Practice*, in *Modern Antenna Handbook*, C. A. Balanis, Ed., chapter 19, John Wiley & Sons, Hoboken, NJ, USA, 2008.
- [5] M. H. Francis, Ed., *IEEE Recommended Practice for Near-Field Antenna Measurements*, IEEE Standard 1720-2012, 2012.
- [6] C. Gennarelli, A. Capozzoli, L. Foged, J. Fordham, and D. J. van Rensburg, Eds., "Recent advances in near-field to far-field transformation techniques," *Int. Jour. Antennas Prop.*, vol. 2012, ID 243203, 2012.
- [7] D. T. Paris, W. M. Leach, Jr., and E. B. Joy, "Basic theory of probe-compensated near-field measurements," *IEEE Trans. Antennas Prop.*, vol. AP-26, pp. 373-379, May 1978.
- [8] E. B. Joy, W. M. Leach, Jr., G. P. Rodrigue, and D. T. Paris, "Application of probe-compensated near-field measurements," *IEEE Trans. Antennas Prop.*, vol. AP-26, pp. 379-389, May 1978.
- [9] Y. Rahmat-Samii, V. Galindo Israel, and R. Mittra, "A plane-polar approach for far-field construction from near-field measurements," *IEEE Trans. Antennas Prop.*, vol. AP-28, pp. 216-230, Mar. 1980.
- [10] Y. Rahmat-Samii and M. S. Gatti, "Far-field patterns of spaceborne antennas from plane-polar near-field measurements," *IEEE Trans. Antennas Prop.*, vol. AP-33, pp. 638-648, June 1985.
- [11] M. S. Gatti and Y. Rahmat-Samii, "FFT applications to plane-polar near-field antenna measurements," *IEEE Trans. Antennas Prop.*, vol. 36, pp. 781-791, June 1988.
- [12] O. M. Bucci, C. Gennarelli, and C. Savarese, "Fast and accurate near-field far-field transformation by sampling interpolation of plane-polar measurements," *IEEE Trans. Antennas Prop.*, vol.



- 39, pp. 48-55, Jan. 1991.
- [13] O. M. Bucci and G. Franceschetti, "On the spatial bandwidth of scattered fields," *IEEE Trans. Antennas Prop.*, vol. AP-35, pp. 1445-1455, Dec. 1987.
- [14] O. M. Bucci, C. Gennarelli, and C. Savarese, "Representation of electromagnetic fields over arbitrary surfaces by a finite and non redundant number of samples," *IEEE Trans. Antennas Prop.*, vol. 46, pp. 351-359, Mar. 1998.
- [15] O. M. Bucci and C. Gennarelli, "Application of nonredundant sampling representations of electromagnetic fields to NF-FF transformation techniques," *Int. Jour. Antennas Prop.*, vol. 2012, ID 319856, 14 pages, 2012.
- [16] F. Ferrara, C. Gennarelli, R. Guerriero, G. Riccio, and C. Savarese, "An efficient near-field to far-field transformation using the planar wide-mesh scanning," *Jour. Electr. Waves Appl.*, vol. 21, pp. 341-357, 2007.
- [17] F. D'Agostino, I. De Colibus, F. Ferrara, C. Gennarelli, R. Guerriero, and M. Migliozi, "Far-field pattern reconstruction from near-field data collected via a nonconventional plane-rectangular scanning: Experimental testing," *Int. Jour. Antennas Prop.*, vol. 2014, ID 763687, 9 pages, 2014.
- [18] O. M. Bucci, C. Gennarelli, G. Riccio, and C. Savarese, "Near-field - far-field transformation from nonredundant plane-polar data: effective modellings of the source," *IEE Proc. Microw., Antennas Prop.*, vol. 145, pp. 33-38, Feb. 1998.
- [19] O. M. Bucci, F. D'Agostino, C. Gennarelli, G. Riccio, and C. Savarese, "NF-FF transformation with plane-polar scanning: Ellipsoidal modelling of the antenna," *Automatika*, vol. 41, pp. 159-164, 2000.
- [20] O. M. Bucci, C. Gennarelli, G. Riccio, and C. Savarese, "Fast and accurate far-field evaluation from a non redundant, finite number of plane-polar measurements," *Proc. of 1994 IEEE AP-S Int. Symp.*, Seattle, USA, pp. 540-543, June 1994.
- [21] A. D. Yaghjian, "Antenna coupling and near-field sampling in plane-polar coordinates," *IEEE Trans. Antennas Prop.*, vol. 40, pp. 304-312, Mar. 1992.
- [22] A. D. Yaghjian and M. B. Woodworth, "Sampling in plane-polar coordinates," *IEEE Trans. Antennas Prop.*, vol. 44, pp. 696-700, May 1996.
- [23] F. D'Agostino, F. Ferrara, C. Gennarelli, R. Guerriero, and M. Migliozi, "Far-field pattern reconstruction from a nonredundant plane-polar near-field sampling arrangement: Experimental testing," *IEEE Antennas Wireless Prop. Lett.*, vol. 15, pp. 1345-1348, 2016.
- [24] O. M. Bucci, G. D'Elia, and M. D. Migliore, "Advanced field interpolation from plane-polar

samples: Experimental verification," *IEEE Trans. Antennas Prop.*, vol. 46, pp. 204-210, Feb. 1998.

- [25] A. D. Yaghjian, "Approximate formulas for the far field and gain of open-ended rectangular waveguide," *IEEE Trans. Antennas Prop.*, vol. AP-32, pp. 378-384, Apr. 1984.
- [26] F. D'Agostino, F. Ferrara, C. Gennarelli, R. Guerriero, and M. Migliozi, "An efficient NF-FF transformation technique with plane-polar scanning: Experimental assessments," in *Proc. of LAPC '14*, Loughborough, UK, pp. 231-235, Nov. 2014.



**Francesco D'Agostino** was born near Salerno (Italy) in 1965. He received the Laurea degree in Electronic Engineering from the University of Salerno in 1994, where in 2001 he received the Ph.D. degree in Information Engineering. From 2002 to 2005 he was Assistant Professor at the Engineering Faculty of the University of Salerno where, in October 2005, he was appointed Associate Professor of Electromagnetics and joined the Department of Industrial Engineering, where he is currently working. His research activity includes application of sampling techniques to electromagnetics and to innovative NF-FF transformations, diffraction problems radar cross section evaluations, Electromagnetic Compatibility. In this area, D'Agostino has co-authored 4 books and over 150 scientific papers, published in peer-reviewed international journals and conference proceedings. He is a regular Reviewer for several journals and conferences and has chaired some international events and conferences. D'Agostino is a Member of AMTA, EurAAP, and IEEE.



**Flaminio Ferrara** was born near Salerno, Italy, in 1972. He received the Laurea degree in Electronic Engineering from the University of Salerno in 1999. Since the same year, he has been with the Research Group in Applied Electromagnetics at the University of Salerno. He received the Ph.D. degree in Information Engineering at the same University, where he is presently an Assistant Professor of Electromagnetic Fields. His interests include: application of sampling techniques to the efficient reconstruction of electromagnetic fields and to NF-FF transformation techniques; monostatic radar cross section evaluations of corner reflectors. Ferrara is co-author of more than 180 scientific papers, mainly in international journals and conference proceedings. He is Reviewer for several

international journals and Member of the Editorial board of the International Journal of Antennas and Propagation. He is Member of the IEEE society.



**Claudio Gennarelli** was born in Avellino, Italy, in 1953. He received the Laurea degree (*summa cum laude*) in Electronic Engineering from the University of Naples, Italy, in 1978. From 1978 to 1983, he worked with the Research Group in Electromagnetics at the Electronic Engineering Department of the University “Federico II” of Naples. In 1983, he became Assistant Professor at the Istituto Universitario Navale (IUN), Naples. In 1987, he was appointed Associate Professor of Antennas, formerly at the Engineering Faculty of Ancona University and subsequently at the Engineering Faculty of Salerno University. In 1999, he has been appointed Full Professor at the same University. The main topics of his scientific activity are: reflector antennas analysis, antenna measurements, diffraction problems, radar cross section evaluations, scattering from surface impedances, application of sampling techniques to electromagnetics and to NF–FF transformations. Gennarelli is co-author of more than 370 scientific papers, mainly in international journals and conference proceedings. In particular, he is co-author of four books on NF–FF transformation techniques. He is a Senior Member of the IEEE and Member of the Editorial board of the Open Electrical and Electronic Engineering Journal and of the International Journal of Antennas and Propagation.



**Rocco Guerriero** received the Laurea degree in Electronic Engineering and the Ph.D. degree in Information Engineering from the University of Salerno in 2003 and 2007, respectively. Since 2003, he has been with the Research Group in Applied Electromagnetics of University of Salerno, where he is currently an Assistant Professor of

Electromagnetic Fields. His interests include: application of sampling techniques to the efficient reconstruction of electromagnetic fields and to near-field-far-field transformation techniques; antenna measurements; inversion of ill-posed electromagnetic problems; analysis of microstrip reflectarrays; diffraction problems. Guerriero is co-author of more than 135 scientific papers, mainly in international journals and conference proceedings. He is Reviewer for several international journals and Member of the Editorial board of the International Journal of Antennas and Propagation. Since 2015, he is Member IEEE.



**Massimo Migliozi** received the Laurea degree in Electronic Engineering from the University of Salerno, in 1999. He received the Ph.D. degree in Information Engineering at the same University, where at the present time he is a Research Fellow in Electromagnetic Fields. His scientific interests include: application of sampling techniques to the efficient reconstruction of electromagnetic fields and to NF–FF transformation techniques; antenna measurements; electromagnetic compatibility; antenna design; diffraction problems. Migliozi is co-author of about 100 scientific papers, mainly in international journals and conference proceedings and Reviewer for several international journals.